

## Weinberg's Higgs portal confronting recent LUX and LHC results together with upper limits on $B^+$ and $K^+$ decay into invisibles

Luis A. Anchordoqui,<sup>1</sup> Peter B. Denton,<sup>2</sup> Haim Goldberg,<sup>3</sup> Thomas C. Paul,<sup>1,3</sup>  
 Luiz H. M. da Silva,<sup>1</sup> Brian J. Vlcek,<sup>1</sup> and Thomas J. Weiler<sup>2</sup>

<sup>1</sup>*Department of Physics,  
 University of Wisconsin-Milwaukee, Milwaukee, WI 53201, USA*

<sup>2</sup>*Department of Physics and Astronomy,  
 Vanderbilt University, Nashville TN 37235, USA*

<sup>3</sup>*Department of Physics,  
 Northeastern University, Boston, MA 02115, USA*

(Dated: December 2013)

### Abstract

We discuss a number of experimental constraints on Weinberg's Higgs portal model. In this framework, the standard model (SM) particle spectrum is extended to include one complex scalar field  $S$  and one Dirac fermion  $\psi$ . These new fields are singlets under the SM gauge group and are charged under a global  $U(1)$  symmetry. Breaking of this  $U(1)$  symmetry results in a massless Goldstone boson  $\alpha$  and a massive  $CP$ -even scalar  $r$ , and splits the Dirac fermion into two new mass-eigenstates  $\psi_{\pm}$ , corresponding to Majorana fermions. The interest on such a minimal SM extension is twofold. On the one hand, if the Goldstone bosons are in thermal equilibrium with SM particles until the era of muon annihilation their contribution to the effective number of neutrino species can explain the hints from cosmological observations of extra relativistic degrees of freedom at the epoch of last scattering. On the other hand, the lightest Majorana fermion  $\psi_{-}$  provides a plausible dark matter candidate. Mixing of  $r$  with the Higgs doublet  $\phi$  is characterized by the mass of hidden scalar  $m_h$  and the mixing angle  $\theta$ . We constrain this parameter space using a variety of experimental data, including heavy meson decays with missing energy, the invisible Higgs width, and direct dark matter searches. We show that different experimental results compress the allowed parameter space in complementary ways, covering a large range of  $\psi_{-}$  masses ( $5 \text{ GeV} \lesssim m_{-} \lesssim 100 \text{ GeV}$ ). Though current results narrow the parameter space significantly (for the mass range of interest,  $\theta \lesssim 10^{-3}$  to  $10^{-4}$ ), there is still room for discovery ( $\alpha$  decoupling at the muon annihilation era requires  $\theta \gtrsim 10^{-5}$  to  $10^{-4}$ ). In the near future, measurements from ATLAS, CMS, LHCb, NA62, XENON1T, LUX, and CDMSlite will probe nearly the full parameter space.

## I. INTRODUCTION

With the success of the Large Hadron Collider (LHC) at CERN, a new era of discovery has begun. The  $SU(3)_C \times SU(2)_L \times U(1)_Y$  standard model (SM) of electroweak and strong interactions has once again endured intensive scrutiny, with a dataset corresponding to an integrated luminosity of  $\approx 20 \text{ fb}^{-1}$  of  $pp$  collisions at  $\sqrt{s} = 8 \text{ TeV}$ . Most spectacularly, the recent discovery [1, 2] of a particle which seems to be the SM Higgs has possibly plugged the final remaining experimental hole in the SM, cementing the theory further. The LHC8 data have not yet turned up any evidence of physics beyond the SM [3].

Despite the resilience of the SM, it seems clear that there is more to the story. The concordance model of cosmology – a flat expanding universe comprising 5% baryons, 20% dark matter, and 75% dark energy – is achieving an ever-firmer footing thanks to observations of the Supernova Cosmology Project [4–6], the Supernova Search Team [7–9], the Wilkinson Microwave Anisotropy Probe (WMAP) [10–12], the Hubble Space Telescope [13, 14], the Sloan Digital Sky Survey (SDSS) [15–18], and the Planck spacecraft [19]. These observations are propounding evidence that a description of the physics of the early universe, and thus the particle physics interactions at sub-fermi distances, will require new theoretical concepts which transcend the SM.

The existence of dark matter (DM), has been solidified by multiple astrophysical observations [20]. Weakly interacting massive particles (WIMPs) are among the best motivated candidates [21]. If stable particles with mass and annihilation cross section set by the weak scale exist, they would be produced and annihilate in thermal equilibrium in the early Universe. As the Universe expands, these particles fall out of equilibrium and their number density is frozen in. A typical weak scale interaction rate yields a thermally-averaged WIMP annihilation cross section,  $\langle\sigma v_M\rangle \sim 10^{-9} \text{ GeV}^{-2}$ , which naturally produces a WIMP relic density  $h^2\Omega_{\text{WIMP}} \sim 10^{-10} \text{ GeV}^{-2}/\langle\sigma v_M\rangle$  [22–26] consistent with the measured DM abundance  $h^2\Omega_{\text{DM}} = 0.111(6)$  [27], thus making WIMPs promising candidates of DM.<sup>1</sup>

Since WIMPs are subject to the weak interaction, it is possible to search for them via direct detection experiments,  $\gamma$ -ray observatories, neutrino telescopes, and particle colliders. The first direct detection experiment to claim evidence for DM was DAMA/LIBRA [28], which has recorded an annual modulation in nuclear recoil event rate at the  $8.9\sigma$  level [29]. This modulation can be interpreted as a consequence of the change in the relative motion of the detector through the sea of DM as the Earth rotates around the Sun [30, 31]. Other direct detection experiments have provided supporting evidence for WIMP interactions, including CRESST [32], CoGeNT [33–35], and most recently the CDMS II [36] experiment. Interestingly, all of these observations favor a light WIMP, with mass  $\sim 10 \text{ GeV}$  and an interaction with protons via spin-independent elastic scattering with a cross-section  $\sim 10^{-41} \text{ cm}^2$ . In contrast, the XENON-10 [37] and XENON-100 [38] DM experiments have reported limits which exclude the mass and cross-section regime favored by CoGeNT, CRESST and CDMS II.

A variety of models were employed to reconcile hints of the signals mentioned above with the exclusion from XENON-10 and XENON-100. However, tension has increased even further after recent CDMSlite (for CDMS Low Ionization Threshold Experiment) [39] and

---

<sup>1</sup> Throughout this work we adopt the usual convention of writing the Hubble constant at the present day as  $H_0 = 100 h \text{ km s}^{-1} \text{ Mpc}^{-1}$ . For  $t = \text{today}$ , the various energy densities are expressed in units of the critical density  $\rho_c$ ; *e.g.*, the DM density  $\Omega_{\text{DM}} \equiv \rho_{\text{DM}}/\rho_c$ .

LUX [40] results. At this point only the xenophobic isospin violating dark matter [41–45], with a neutron to proton coupling ratio of  $-0.7$  allows any overlap with the 68% favored contour of CDMS II [46–48]. Favored regions of all other experiments remain excluded.

Adding to the story, the most recent data from WMAP [11, 12], the Atacama Cosmology Telescope [49], and the South Pole Telescope [50] have hinted at a higher value of the fractional energy density in relativistic species than previously estimated [51, 52]. Furthermore, recent estimates of light-element abundances probing Big Bang nucleosynthesis also suggest additional relativistic degrees of freedom in the early Universe [53].

The energy density stored in relativistic species is customarily given in terms of the number of equivalent light neutrino species,

$$N_{\text{eff}} \simeq \frac{8}{7} \sum_{\text{b}}' g_{\text{b}} \left( \frac{T_{\text{b}}}{T_{\nu}} \right)^4 + \sum_{\text{f}}' g_{\text{f}} \left( \frac{T_{\text{f}}}{T_{\nu}} \right)^4, \quad (1)$$

where  $g_{\text{b(f)}}$  are the number of boson (fermion) helicity states,  $T_{\text{b(f)}}$  are the temperatures of the various species, and the primes indicate that electrons and photons are excluded from the sums [54]. The normalization of  $N_{\text{eff}}$  is such that it gives  $N_{\text{eff}} = 3$  for three families of massless left-handed SM neutrinos, with temperature  $T_{\nu}$ .

The latest chapter in the story is courtesy of the Planck spacecraft. Unexpectedly, the best multi-parameter fit of Planck data yields a Hubble constant  $h = 0.674 \pm 0.012$  [19], a result which deviates by more than  $2\sigma$  from the value obtained with the Hubble Space Telescope,  $h = 0.738 \pm 0.024$  [14]. The impact of the Planck  $h$  estimate is particularly important in the determination of  $N_{\text{eff}}$ . Combining observations of the cosmic microwave background (CMB) with data from baryon acoustic oscillations, the Planck Collaboration reported  $N_{\text{eff}} = 3.30 \pm 0.27$  [19]. However, a combination of the space telescope measurement  $h = 0.738 \pm 0.024$  with the Planck CMB data gives  $N_{\text{eff}} = 3.62 \pm 0.25$ , which suggests new neutrino-like physics (at around the  $2.3\sigma$  level) [19].

As alluded to already, beyond SM physics may be required to resolve these tensions. The Higgs sector could provide the promising territory to introduce new physics, as the couplings are the least experimentally constrained at present. Perhaps the most direct example is the Higgs portal, which connects the SM Higgs to a scalar field in a hidden sector by an elementary quartic interaction [55–58]. One realization of this concept has been introduced recently by Weinberg specifically to address the apparent inconsistencies between the cosmological and astrophysical measurements discussed above [59]. In this framework the SM is extended by one complex scalar field  $S$  and one Dirac fermion field  $\psi$ . The new fields are singlets under the SM gauge group and are charged under a global  $U(1)_W$  symmetry, namely:  $U(1)_W(\psi) = 1$  and  $U(1)_W(S) = 2$ . Of course, all the SM fields transform trivially under the global symmetry. The spontaneous breaking of this global symmetry gives rise to a massless Goldstone boson and a  $CP$ -even scalar, and splits the Dirac fermion into two new mass-eigenstates  $\psi_{\pm}$ , corresponding to Majorana fermions. If the Goldstone bosons are in thermal equilibrium with the SM particles until the era of muon annihilation, then they can contribute to the effective number of neutrino species. Furthermore the symmetry breaking leads naturally to a dark matter candidate. Fields with an even (odd) charge under the global  $U(1)$  symmetry will acquire, after symmetry breaking, an even (odd) discrete charge under a  $Z_2$  discrete symmetry. While the SM particles are all even under  $Z_2$ , the Majorana fermions  $\psi_{\pm}$  are odd. The lightest particle with odd charge,  $\psi_{-}$ , will be absolutely stable, and thus a plausible dark matter candidate.

In this paper we explore the plausible parameter space of this model. The outline is as follows. In Sec. II we describe the main characteristics of Weinberg’s Higgs portal model. In Sec. III we study the contributions to the effective number of neutrino species in the plane spanned by the mixing angle between scalars in the visible and hidden sectors and the mass of the  $CP$ -even scalar. In Sec. IV we use collider data to constrain this parameter space via processes involving the hidden scalar. In Sec. V we use data from direct dark matter searches to further constrain the parameter space via the hidden fermions. In Sec. VI we explore the impact of LHC measurements of the invisible width of the Higgs on the same parameter space. In Sec. VII we gather our conclusions.

## II. WEINBERG’S HIGGS PORTAL MODEL

The Higgs portal couples a complex singlet field  $S$  to the SM doublet  $\Phi$ , through which the singlet field interacts with the SM. The renormalizable Lagrangian density of the model is

$$\mathcal{L} = \partial_\mu S^\dagger \partial^\mu S + \mu^2 S^\dagger S - \lambda(S^\dagger S)^2 - g_\theta (S^\dagger S)(\Phi^\dagger \Phi) + \mathcal{L}_{\text{SM}}, \quad (2)$$

where  $\mu$ ,  $\lambda$ , and  $g_\theta$  are constants and  $\mathcal{L}_{\text{SM}}$  is the usual SM Lagrangian. The Higgs sector in  $\mathcal{L}_{\text{SM}}$  is given by

$$\mathcal{L}_{\text{SM}} \supset (D_\mu \Phi)^\dagger (D^\mu \Phi) + \mu_{\text{SM}}^2 \Phi^\dagger \Phi - \lambda_{\text{SM}}(\Phi^\dagger \Phi)^2. \quad (3)$$

Following Weinberg, we write  $S$  in terms of two real fields (its massive radial component and a massless Goldstone boson). The radial field develops a VEV  $\langle r \rangle$  about which the field  $S$  is expanded

$$S = \frac{1}{\sqrt{2}} (\langle r \rangle + r(x)) e^{i2\alpha(x)}. \quad (4)$$

The phase of  $S$  is adjusted to make  $\langle \alpha(x) \rangle = 0$ . In the unitary gauge the Higgs doublet is expanded around the VEV as

$$\Phi(x) = \frac{1}{\sqrt{2}} \begin{pmatrix} 0 \\ \langle \phi \rangle + \phi(x) \end{pmatrix}, \quad (5)$$

with  $\langle \phi \rangle = 246$  GeV. The fields  $\phi$  and  $r$ , under the influence of the  $g_\theta$ -term, mix and become two physical massive Higgs fields [60]

$$\begin{pmatrix} h \\ H \end{pmatrix} = \begin{pmatrix} \cos \theta & -\sin \theta \\ \sin \theta & \cos \theta \end{pmatrix} \begin{pmatrix} r \\ \phi \end{pmatrix} \quad (6)$$

with masses

$$m_h = \lambda \langle r \rangle^2 + \lambda_{\text{SM}} \langle \phi \rangle^2 - \sqrt{(\lambda_{\text{SM}} \langle \phi \rangle^2 - \lambda \langle r \rangle^2)^2 + g_\theta^2 \langle r \rangle^2 \langle \phi \rangle^2} \quad (7)$$

and

$$m_H = \lambda \langle r \rangle^2 + \lambda_{\text{SM}} \langle \phi \rangle^2 + \sqrt{(\lambda_{\text{SM}} \langle \phi \rangle^2 - \lambda \langle r \rangle^2)^2 + g_\theta^2 \langle r \rangle^2 \langle \phi \rangle^2}, \quad (8)$$

and mixing angle

$$\tan 2\theta = \frac{g_\theta \langle r \rangle \langle \phi \rangle}{\lambda_{\text{SM}} \langle \phi \rangle^2 - \lambda \langle r \rangle^2}. \quad (9)$$

The small  $\theta$  limit leads to the usual SM phenomenology with an isolated hidden sector.

Adding in the dark matter sector requires at least one Dirac field

$$\mathcal{L}_\psi = i\bar{\psi}\gamma \cdot \partial\psi - m_\psi\bar{\psi}\psi - \frac{f}{\sqrt{2}}\bar{\psi}^c\psi S^\dagger - \frac{f^*}{\sqrt{2}}\bar{\psi}\psi^c S. \quad (10)$$

As advanced in the Introduction, we assign to the hidden fermion a charge  $U(1)_W(\psi) = 1$ , so that the Lagrangian is invariant under the global transformation  $e^{iW\alpha}$ . Treating the transformation as local allows us to express  $\psi$  as

$$\psi(x) = \psi'(x)e^{i\alpha(x)}. \quad (11)$$

Once the radial field achieves a VEV we can expand the dark matter sector to get

$$\begin{aligned} \mathcal{L}_\psi &= \frac{i}{2} \left( \bar{\psi}'\gamma \cdot \partial\psi' + \bar{\psi}'^c\gamma \cdot \partial\psi'^c \right), \\ &- \frac{m_\psi}{2} (\bar{\psi}'\psi' + \bar{\psi}'^c\psi'^c) - \frac{f\langle r \rangle}{2} \bar{\psi}'^c\psi' - \frac{f\langle r \rangle}{2} \bar{\psi}'\psi'^c, \\ &- \frac{1}{2} (\bar{\psi}'\gamma\psi' - \bar{\psi}'^c\gamma\psi'^c) \cdot \partial\alpha, \\ &- \frac{f}{2} r (\bar{\psi}'^c\psi' + \bar{\psi}'\psi'^c). \end{aligned} \quad (12)$$

Diagonalization of the  $\psi'$  mass matrix generates the mass eigenvalues,

$$m_\pm = m_\psi \pm f\langle r \rangle, \quad (13)$$

for the two mass eigenstates

$$\psi_- = \frac{i}{\sqrt{2}} (\psi'^c - \psi') \quad \text{and} \quad \psi_+ = \frac{1}{\sqrt{2}} (\psi'^c + \psi'). \quad (14)$$

In this basis, the act of charge conjugation on  $\psi_\pm$  results in

$$\psi_\pm^c = \psi_\pm. \quad (15)$$

This tells us that the fields  $\psi_\pm$  are Majorana fermions. The Lagrangian is found to be

$$\begin{aligned} \mathcal{L}_\psi &= \frac{i}{2} \bar{\psi}_+\gamma \cdot \partial\psi_+ + \frac{i}{2} \bar{\psi}_-\gamma \cdot \partial\psi_- - \frac{1}{2} m_+ \bar{\psi}_+\psi_+ - \frac{1}{2} m_- \bar{\psi}_-\psi_-, \\ &- \frac{i}{4\langle r \rangle} (\bar{\psi}_+\gamma\psi_- - \bar{\psi}_-\gamma\psi_+) \cdot \partial\alpha', \\ &- \frac{f}{2} r (\bar{\psi}_+\psi_+ - \bar{\psi}_-\psi_-), \end{aligned} \quad (16)$$

where  $\alpha' \equiv 2\alpha\langle r \rangle$  is the canonically normalized Goldstone boson. We must now put  $r$  into its massive field representation, for which the interactions of interest are

$$- \frac{f \sin \theta}{2} H (\bar{\psi}_+\psi_+ - \bar{\psi}_-\psi_-) - \frac{f \cos \theta}{2} h (\bar{\psi}_+\psi_+ - \bar{\psi}_-\psi_-). \quad (17)$$

This leads to 3-point interactions between the Majorana fermions and the Higgs boson of the SM.

In summary, the Dirac fermion of the hidden sector splits into two Majorana mass-eigenstates. The heavier state will decay into the lighter one by emitting a Goldstone boson. The lighter one, however, is kept stable by the unbroken reflection symmetry. Therefore, we can expect that the universe today will contain only one type of Majorana WIMP, the lighter one  $w$ , with mass  $m_w$  equal to the smaller of  $m_{\pm}$ . The dark sector hence contains five unknown parameters,  $m_w$ ,  $m_h$ ,  $\lambda$ ,  $\theta$ , and  $f$ . To avoid fine tuning herein we impose an additional constraint relating some of these free parameters:  $\Delta m/m_w \ll 1$ , where  $\Delta m = |m_+ - m_-| = 2|f\langle r \rangle|$ .

### III. GOLDSTONE BOSONS AS IMPOSTER FRACTIONAL NEUTRINOS

In the early Universe, the Goldstone bosons were at thermal equilibrium with the SM particles. As the Universe cooled due to its Hubble expansion,  $H(T) \simeq 1.66\sqrt{g(T)}T^2/M_{\text{Pl}}$ , the weakly interacting Goldstone bosons decoupled from the SM particles. Throughout  $M_{\text{Pl}}$  is the Planck mass and  $g(T)$  is the effective number of interacting (thermally coupled) relativistic degrees of freedom at temperature  $T$ . Following Weinberg we require that the  $\alpha$ 's go out of equilibrium when the temperature is about the muon mass,  $T_{\alpha'}^{\text{dec}} \approx m_{\mu} \simeq 105$  MeV, ensuring that

$$N_{\text{eff}} = 3 + (4/7)(43/57)^{4/3} = 3.39. \quad (18)$$

For  $0.2 \text{ GeV} \lesssim m_h \lesssim 4 \text{ GeV}$ , the interaction rate of Goldstone bosons is dominated by resonant annihilation into fermion-antifermion pairs [61]. The  $\alpha\alpha \rightarrow \bar{f}f$  rate is given by

$$\Gamma(T) = \frac{g_{\theta}^2}{256 \pi} \frac{m_h^6}{m_H^4 \Gamma_h} \frac{K_2(m_h/T)}{T^2} \sum_f m_f^2 \left(1 - \frac{4m_f^2}{m_h^2}\right)^{3/2}, \quad (19)$$

where  $K_2(x)$  is the 2<sup>nd</sup> Modified Bessel function of the second kind and  $\Gamma_h$  is the decay width of the  $CP$ -even scalar; see Appendix A for details. Note that since the interaction rate is proportional to the fermion square mass, in (19) it is enough to consider only the annihilation into  $\mu^{\pm}$  pairs. Enforcing the decoupling condition,  $\Gamma(T_{\alpha'}^{\text{dec}}) = H(T_{\alpha'}^{\text{dec}})$ , we obtain

$$\frac{M_{\text{Pl}} g_{\theta}^2}{256 \pi} \frac{m_h^6}{m_H^4 \Gamma_h} \frac{K_2(m_h/m_{\mu})}{m_{\mu}^2} \left(1 - \frac{4m_{\mu}^2}{m_h^2}\right)^{3/2} \approx 6.28. \quad (20)$$

For  $m_h < 2m_w$ , the decay width is given by [60]

$$\Gamma_h = \frac{m_h^3}{32 \pi \langle r \rangle^2} \approx \frac{m_h}{16\pi} \lambda. \quad (21)$$

Using (9) we obtain an expression for the decoupling condition relating the two unknown parameters

$$\sin \theta \approx \frac{8 \sqrt{6.28} m_H^2 m_h \langle \phi \rangle}{\sqrt{8} M_{\text{Pl}} m_{\mu} |m_H^2 - m_h^2| m_{\mu}} \left[ \frac{m_h}{m_{\mu}} \left( \frac{m_h^2}{m_{\mu}^2} - 4 \right)^{3/4} K_2^{1/2}(m_h/m_{\mu}) \right]^{-1}. \quad (22)$$

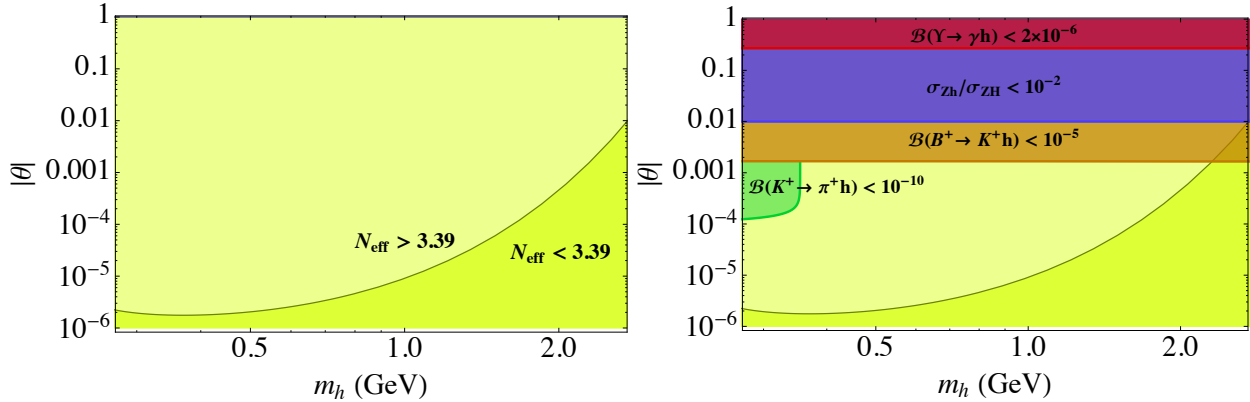


FIG. 1: **Left:** Contour of constant  $N_{\text{eff}} = 3.39$  in the  $(|\theta|, m_h)$  plane. **Right:** Bounds from interactions involving SM particles in the initial state and the  $CP$ -even scalar in the final state, overlaid on the same plane.

In Fig. 1 we show, in the  $(|\theta|, m_h)$  plane, the contour which corresponds to  $N_{\text{eff}} = 3.39$ . This particular choice of the number of effective neutrino species is midway between the value reported by the Planck Collaboration using their best determination of  $h$  and the value determined using the  $h$  observed by the Hubble Space Telescope [19]. The interesting region lies above the contour in the sense that physics beyond the SM would be required. In the remainder of the paper we concentrate on constraining this region of the parameter space.

#### IV. CONSTRAINTS FROM THE HIDDEN SCALAR

In the spirit of [62], in this section we evaluate the impact of experimental limits on  $B^+ \rightarrow K^+ + \cancel{E}_T$  reported by the BaBar [63–65], CLEO [66], and BELLE [67] collaborations, as well as limits on  $K^+ \rightarrow \pi^+ + \cancel{E}_T$  from the E787 [68] and E949 experiments [69–71] on the  $(\theta, m_h)$  plane.

Before proceeding, we pause to note that combining the upper limit reported by the BaBar Collaboration  $\mathcal{B}(\Upsilon \rightarrow \gamma + \cancel{E}_T) < 2 \times 10^{-6}$  [72] and the Wilczek mechanism [73] with its one loop QCD correction (which results in  $\approx 84\%$  decrease of the total rate [74–76]), one obtains an upper bound for the mixing angle,  $\theta < 0.27$  [77]. A stronger constraint follows from LEP limits on the production of invisibly-decaying Higgs bosons  $\sigma_{Zh}/\sigma_{ZH} < 10^{-2}$  [78–81], which implies  $\theta < 10^{-2}$  [82].

Searches for the rare flavor-changing neutral-current decay  $B^+ \rightarrow K^+ + \cancel{E}_T$  have been conducted by the BaBar [63–65], CLEO [66], and BELLE [67] collaborations. The corresponding SM mode is a decay into  $K^+$  and a pair of neutrinos, with a branching ratio  $\mathcal{B}(B^+ \rightarrow K^+ \nu \bar{\nu}) \approx 3 \times 10^{-6}$  [83, 84]. No significant excess of such decays over background has been observed. The most stringent upper limit has been reported by the BaBar Collaboration,  $\mathcal{B}(B^+ \rightarrow K^+ + \cancel{E}_T) < 1.3 \times 10^{-5}$ , at 90% C.L. [64]. In our calculation we subtract the SM contribution to the branching fraction to arrive at

$$\mathcal{B}(B^+ \rightarrow K^+ h) < 10^{-5} \quad (23)$$

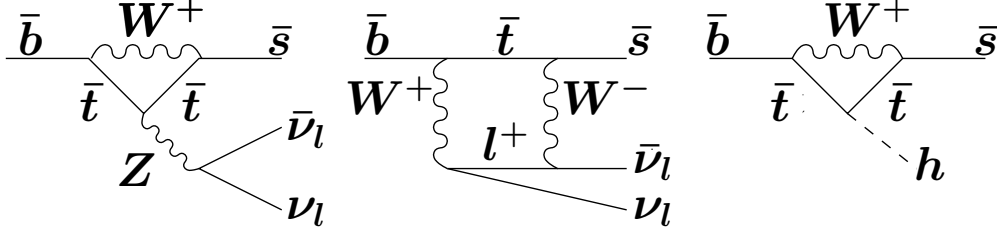


FIG. 2: Feynman diagrams which contribute to  $B$  meson decays with  $\cancel{E}_T$ . The second-order weak processes that contribute to the  $B^+ \rightarrow K^+ \nu \bar{\nu}$  branching ratio are the “ $Z$ -penguin” diagram (left) and the “box” diagram (middle). The hypothetical  $b \rightarrow sh$  transition (right) would also yield a missing energy signal.

to be consistent with existing data at 90% CL.

At the quark level the decays of the  $B^+$  meson with missing energy correspond to the processes shown in Fig. 2. The branching fraction for the decay  $B^+ \rightarrow K^+ h$  is found to be

$$\mathcal{B}(B^+ \rightarrow K^+ h) = \frac{9\sqrt{2}\tau_B G_F^3 m_t^4 m_b^2}{1024\pi^5 m_B^3} |V_{tb}V_{ts}^*|^2 \left[ \frac{(m_B + m_K)(m_B - m_K)}{(m_b - m_s)} f_0^{BK}(m_h^2) \right]^2 \times \sqrt{[(m_B + m_K)^2 - m_h^2][(m_B - m_K)^2 - m_h^2]} \theta^2, \quad (24)$$

where

$$f_0^{BK}(q^2) = 0.33 \exp\left(\frac{0.63q^2}{m_B^2} - \frac{0.095q^4}{m_B^4} + \frac{0.591q^6}{m_B^6}\right) \quad (25)$$

is the form factor [85],  $G_F \approx 1.17 \times 10^{-5}$  GeV $^{-2}$  is the Fermi constant,  $\tau_B = 1.641 \times 10^{-12}$  s is the  $B$ -meson lifetime, and  $m_B = 5.279$  GeV,  $m_K = 0.494$  GeV,  $m_t = 173$  GeV,  $m_b = 4.2$  GeV, and  $m_s = 0.095$  GeV are the corresponding particle masses [27]. The CKM matrix elements yield  $|V_{tb}V_{ts}^*| \approx 0.0389$  [86]. Equating (23) and (24) we obtain an upper limit on the mixing angle

$$\theta^2 < \frac{1024 \pi^5 m_B^3}{9\sqrt{2} \tau_B G_F^3 m_t^4 m_b^2 |V_{tb}V_{ts}^*|^2} \frac{10^{-5}}{\sqrt{[(m_B + m_K)^2 - m_h^2][(m_B - m_K)^2 - m_h^2]}} \mathcal{F}_B, \quad (26)$$

where

$$\mathcal{F}_B = \left[ \frac{(m_B + m_K)(m_B - m_K)}{(m_b - m_s)} f_0^{BK}(m_h^2) \right]^{-2}. \quad (27)$$

Lowering the mass of  $m_h \lesssim 355$  MeV opens the decay channel  $K^+ \rightarrow \pi^+ + \cancel{E}_T$ . Similar to the previous decay process, the decay  $K^+ \rightarrow \pi^+ h$  can proceed through a penguin diagram.<sup>2</sup> The experiment E949 at Brookhaven National Laboratory studied the rare decay  $K^+ \rightarrow \pi^+ \nu \bar{\nu}$  with an exposure of  $1.71 \times 10^{12}$  stopped kaons [69–71]. The data were analyzed using a blind analysis technique yielding five candidate events. Combining this result with the observation of two candidate events by the predecessor experiment E7877 [68] yields the branching ratio  $\mathcal{B}(K^+ \rightarrow \pi^+ \nu \bar{\nu}) = 1.73_{-1.05}^{+1.15} \times 10^{-10}$  [71], which is consistent with the SM

<sup>2</sup> Although this penguin have both flippers it appears to be missing both of its legs.



prediction of  $(7.81_{-0.71}^{+0.80} \pm 0.29) \times 10^{-11}$  (the uncertainties listed first derive from the input parameters, the smaller uncertainties listed second demonstrate the size of the intrinsic theoretical uncertainties) [87–89]. The probability that all seven events were due to background only (background and SM signal) was estimated to be 0.001 (0.073). In our calculation we subtract the SM branching fraction from the experimental observation to get

$$\mathcal{B}(K^+ \rightarrow \pi^+ h) < 10^{-10} \quad (28)$$

in order to be consistent with existing data.

Using (24) with the appropriate replacements for the quark constituents we obtain the branching for  $K^+ \rightarrow \pi^+ h$

$$\begin{aligned} \mathcal{B}(K^+ \rightarrow \pi^+ h) &= \frac{9\sqrt{2}\tau_K G_F^3 m_t^4 m_s^2}{1024\pi^5 m_K^3} |V_{ts}V_{td}^*|^2 \left[ \frac{(m_K + m_\pi)(m_K - m_\pi)}{m_s - m_d} f_0^{K\pi}(m_h^2) \right]^2 \\ &\times \sqrt{[(m_K + m_\pi)^2 - m_h^2][(m_K - m_\pi)^2 - m_h^2]} \theta^2, \end{aligned} \quad (29)$$

where the form factor is given by [90]

$$f_0^{K\pi}(q^2) \approx 0.96 \left( 1 + 0.02 \frac{q^2}{m_\pi^2} \right). \quad (30)$$

Here,  $\tau_K = 1.24 \times 10^{-8}$  s,  $m_\pi = 0.1396$  GeV,  $m_d = 0.0048$  GeV, and  $|V_{ts}V_{td}^*| = 3.07 \times 10^{-4}$ . Equating (28) to (29) we obtain an upper limit on the mixing angle

$$\theta^2 < \frac{1024 \pi^5 m_K^3}{9\sqrt{2} \tau_K G_F^3 m_t^4 m_s^2 |V_{ts}V_{td}^*|^2} \frac{10^{-10}}{\sqrt{[(m_K + m_\pi)^2 - m_h^2][(m_K - m_\pi)^2 - m_h^2]}} \mathcal{F}_K \quad (31)$$

where

$$\mathcal{F}_K = \left[ \frac{(m_K + m_\pi)(m_K - m_\pi)}{(m_s - m_d)} f_0^{K\pi}(m_h^2) \right]^{-2}. \quad (32)$$

In Fig. 1 we summarize these results in the  $(\theta, m_h)$  plane. Note that for  $m_h < 355$  MeV the  $K^+ \rightarrow \pi^+ h$  channel dominates, requiring  $|\theta| < 10^{-4}$ . For  $355 \text{ MeV} < m_h < 2 \text{ GeV}$ , the  $B^+ \rightarrow K^+ h$  dominates, setting an upper bound  $|\theta| < 10^{-3}$ .

It is important to explain the reason the bound derived from  $B$  decay measurements shown in Fig. 1 appears not to depend on  $m_h$ . Recall we are probing regions for which  $0.2 \text{ GeV} \lesssim m_h \lesssim 2 \text{ GeV}$ . For these values, the exponential in the form factor and the denominator with the square root, see Eq. (27), do not vary much with  $m_h$ , since they do not depend directly on  $m_h$  but rather on the ratio  $m_h/m_B$  and  $m_h/(m_B \pm m_K)$ , respectively. Since  $m_B \sim 5.3 \text{ GeV}$ , these ratios are small and there is little variation of the bound with  $m_h$ .

## V. CONSTRAINTS FROM THE HIDDEN FERMIONS

Next, in line with our stated plan, we use data from DM searches at direct detection experiments to constrain the parameter space of the fermion sector. The WIMP-nucleon cross section for scalar interactions is found to be [91].

$$\sigma_{wN} = \frac{4}{\pi} \frac{m_w^2 m_N^4}{(m_w + m_N)^2} f_N^2, \quad (33)$$

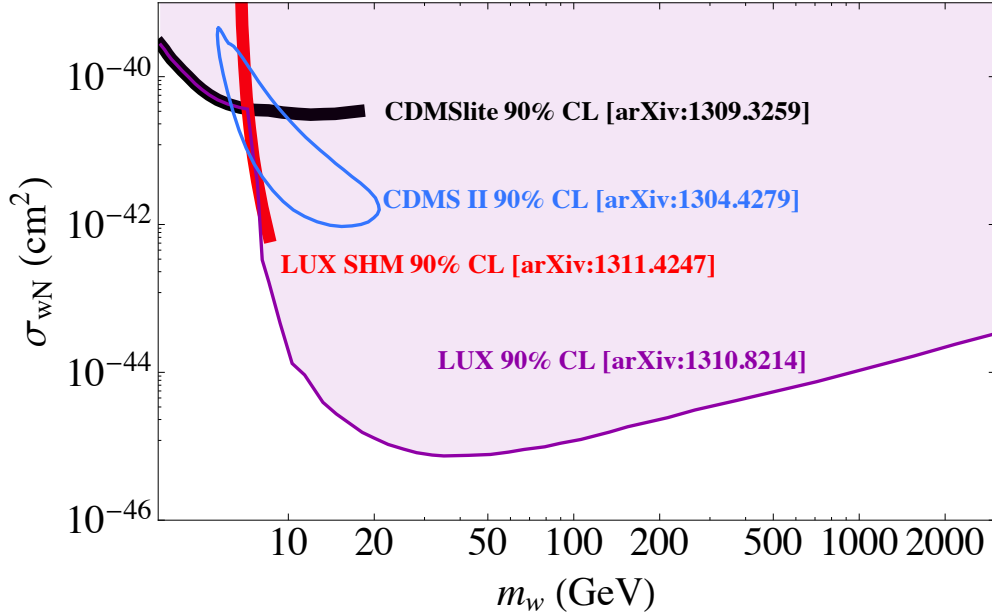


FIG. 3: Favored 90% C.L. region of CDMS II [36], and 90% C.L. exclusion contours of LUX [40], CDMSlite [39], and LUX assuming the standard halo model (SHM) [47] in the  $(\sigma_{wN}, m_w)$  plane.

where  $m_N \simeq 1$  GeV is the nucleon mass and  $f_N$  is the WIMP-nucleon coupling. For the case at hand,

$$f_N \simeq \frac{G_q}{4m_q}, \quad \text{with} \quad \frac{G_q}{m_q} = \frac{2fg_\theta \langle r \rangle}{2\sqrt{2}m_H^2 m_h^2}, \quad (34)$$

yielding [60]

$$\sigma_{wN} = \left( \frac{1}{2\sqrt{2}} \right)^2 \frac{1}{4\pi} \frac{m_w^2 m_N^4}{(m_w + m_N)^2} \left( \frac{2g_\theta \langle r \rangle f}{m_H^2 m_h^2} \right)^2. \quad (35)$$

We may re-express this result in terms of the mixing angle,

$$\sigma_{wN} = (0.35)^2 \frac{1}{4\pi} \frac{m_w^2 m_N^4}{(m_w + m_N)^2} \left( \frac{f}{\langle \phi \rangle} \right)^2 \left( \frac{1}{m_H^2} - \frac{1}{m_h^2} \right)^2 \sin^2 2\theta. \quad (36)$$

For  $\theta \ll 1$ , the upper limits on the nucleon-wimp cross sections derived by the various experiments translate into upper limits of the mixing angle

$$|\theta| < \frac{(m_w + m_N) \langle \phi \rangle}{m_N^2 m_w} \left| \frac{1}{m_H^2} - \frac{1}{m_h^2} \right|^{-1} \frac{\sqrt{\pi}}{0.35} \sqrt{\sigma_{wN}(m_w)}. \quad (37)$$

To determine  $f$  we require the  $w$  relic density to be consistent with  $h^2 \Omega_{\text{DM}} \simeq 0.111(6)$ . In our study we consider the interesting case in which  $m_h < m_w$ , for which threshold and resonant effects are negligible and thus the instantaneous freeze-out approximation is valid [61]. In this region of the parameter space, the  $w$ 's predominantly annihilate into a pair of  $h$ 's or co-annihilate with the next-to-lightest Majorana fermion, producing a scalar  $h$  and a Goldstone boson. All of the final state  $h$ 's subsequently decay into  $\alpha$ 's. We note, however, that for

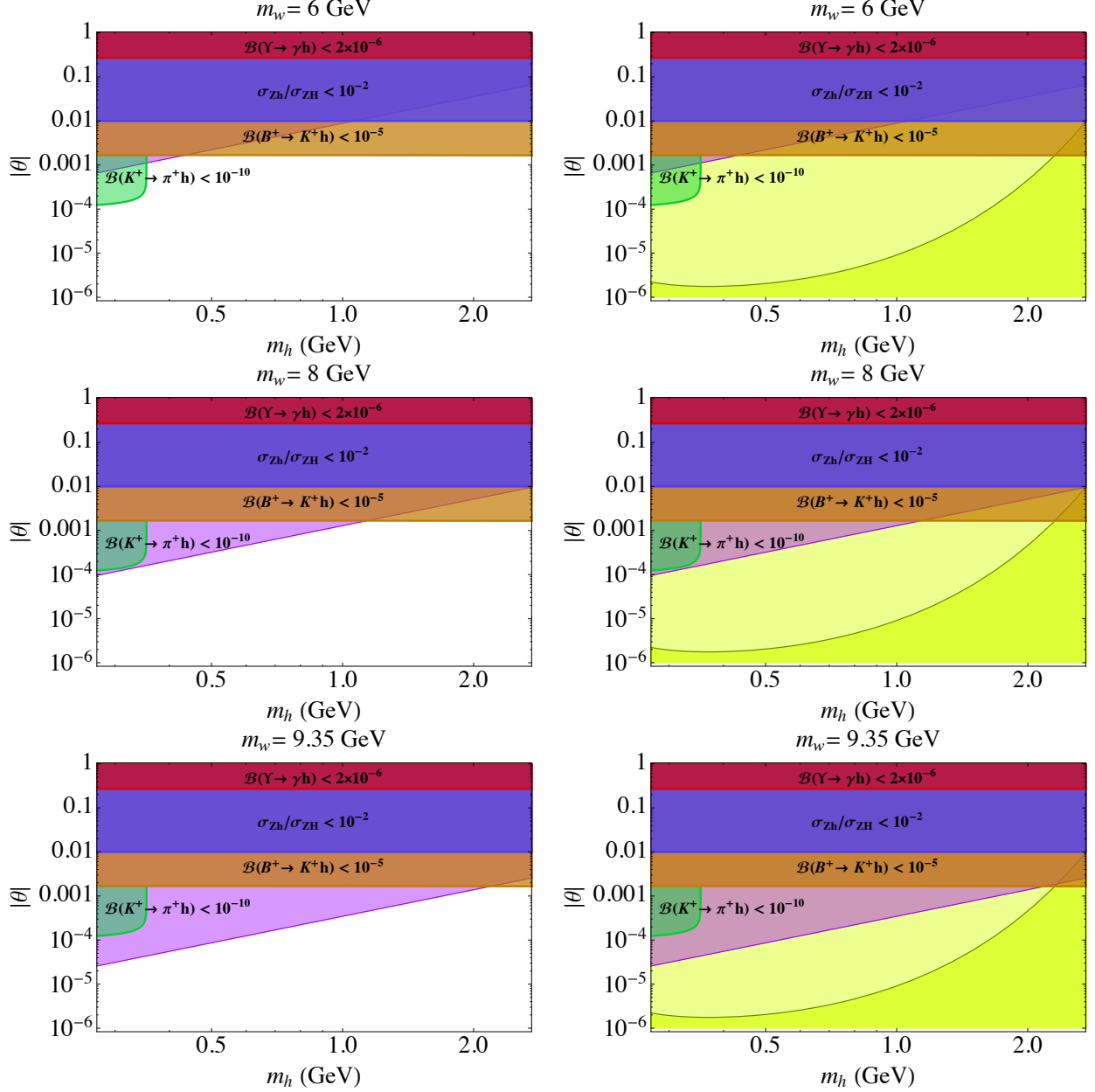


FIG. 4: Plots on the left indicate bounds in the  $(\theta, m_h)$  plan arising from heavy meson decays with missing energy as well as bounds from DM direct detection experiments. On the right, the contour for  $N_{\text{eff}} = 3.39$  is overlaid on the bounds. We have taken  $m_w = 6$  GeV, 8 GeV, and 9.35 GeV.

$m_w \approx m_H/2$  one expects dominant annihilation into fermions. Indeed, resonant annihilation of  $w$  into fermion and subsequent photon production has been proposed as a possible DM signal accesible to  $\gamma$ -ray detectors [60].<sup>3</sup> Interestingly, for  $m_w \simeq 60$  GeV, resonant Higgs production will result in predominantly  $b\bar{b}$  final states, which in turn hadronize to states including photons that may be consistent with the photon flux in the Fermi bubbles [93–96].

<sup>3</sup> An alternative  $\gamma$ -ray signal has been proposed in [92].

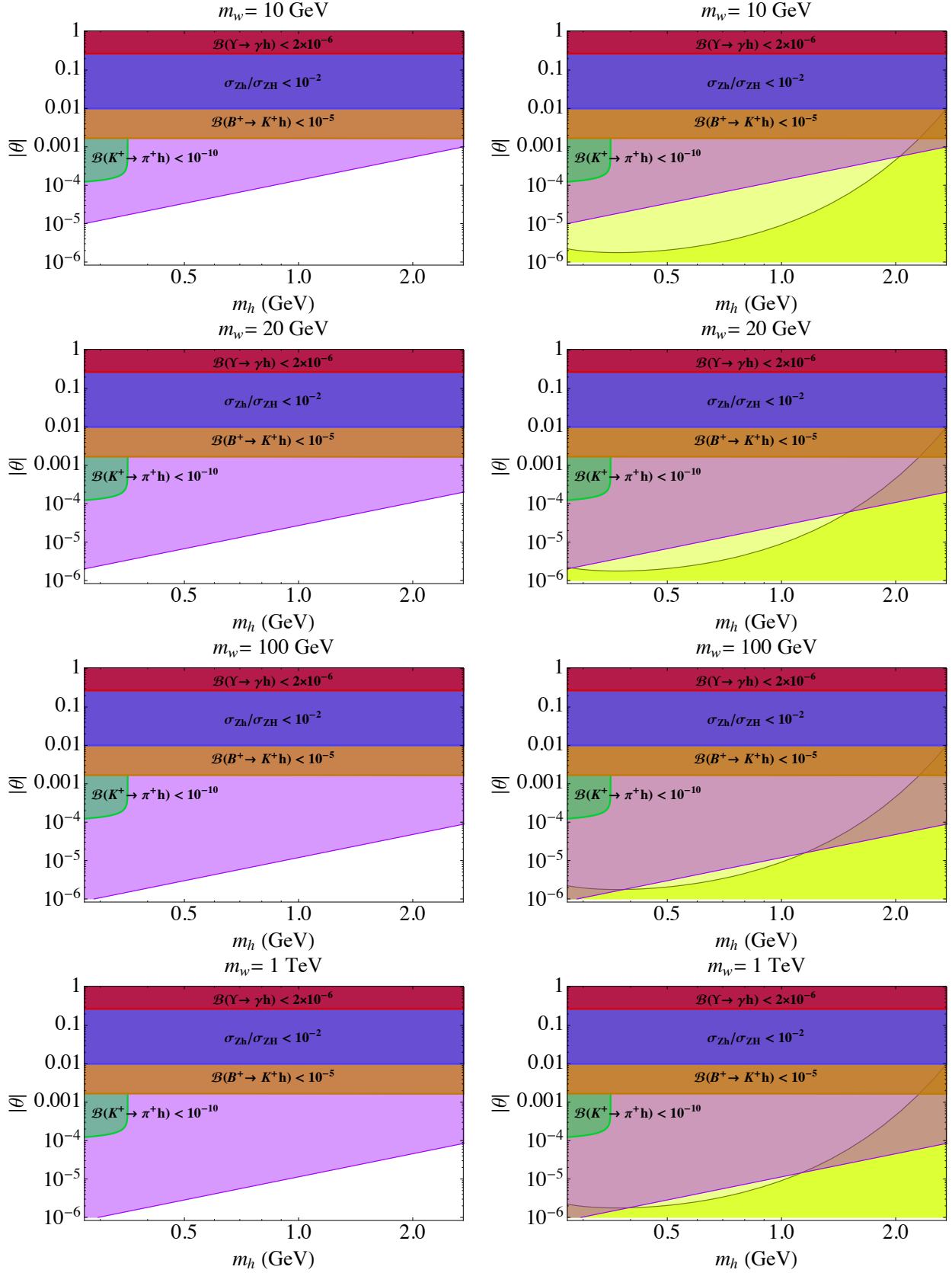


FIG. 5: Idem Fig. 4, but for different values of  $m_w$ .

We compute the thermal-angular average using the Gondolo-Gelmini technique [97],

$$\begin{aligned} \langle \sigma_{ww} v_M \rangle &= \frac{1}{n_w^2(T)} \int \frac{d^3 p_1}{(2\pi)^3} \frac{d^3 p_2}{(2\pi)^3} \sigma_{ww} v_M e^{-E_1/T} e^{-E_2/T} , \\ &= \frac{x_f}{8m_w^5 K_2^2(x_f)} \int_{4m_w^2}^{\infty} \sigma_{ww}(s) \sqrt{s}(s - 4m_w^2) K_1(x_f \sqrt{s}/m_w) ds , \end{aligned} \quad (38)$$

where  $x_f = m_w/T_f$ , with  $T_f$  the freeze-out temperature. It is easily seen that [61]

$$\lim_{\Delta m/m_w \rightarrow 0} \langle \sigma_{ww} v_M \rangle \approx \frac{f^4}{32\pi m_w^2} . \quad (39)$$

The freeze out analysis of the Boltzmann equation gives,

$$\langle \sigma_{ww} v_M(x_f) \rangle = \frac{1.04 \times 10^9 x_f}{\sqrt{g(x_f)} M_{\text{Pl}} \Omega_{\text{DM}} h^2} \text{ GeV}^{-1} , \quad (40)$$

which, for pedagogical reasons, is derived in detail in Appendix B. Combining (39) and (40) we obtain

$$\frac{f^4}{32\pi m_w^2} = \frac{1.04 \times 10^9 \text{ GeV}^{-1} x_f}{\sqrt{g(x_f)} M_{\text{Pl}} \Omega_{\text{DM}} h^2} , \quad (41)$$

or equivalently

$$f \approx \left( \frac{1.04 \times 10^{11} \text{ GeV}^{-1} x_f}{\sqrt{g(x_f)} M_{\text{Pl}} \Omega_{\text{DM}} h^2} \right)^{1/4} \sqrt{m_w} . \quad (42)$$

Since the WIMPs couple to the SM via the Higgs, the model is isospin-invariant.<sup>4</sup> Thus, to determine bounds on the  $(|\theta|, m_h)$  parameter space, we consult the experimental limits on the WIMP nucleon cross section shown in Fig. 3. Placing these limits in (37) together with the value of  $f$  derived from the requirement that the relic density is correctly reproduced, we extract limits on  $|\theta|$ , as shown in Figs. 4 and 5. Once  $m_w$  exceeds 8 GeV, the bounds from direct detection experiments begin to constrain the parameter space. For  $m_w > 9.35$  GeV the bounds from direct detection dominate over the bounds from the interactions involving the  $CP$ -even scalar. Recall that this analysis does not account for excitations of the SM Higgs, which prevents us from using this technique to probe regions where  $55 \text{ GeV} \lesssim m_w \lesssim 70 \text{ GeV}$ . For  $m_w > 100$  GeV, the region requiring new physics has been nearly excluded.

## VI. CONSTRAINTS FROM HIGGS DECAY INTO INVISIBLES

As we remarked in the Introduction, the LHC has ushered in a new era of discovery, with confirmation of the reality of the SM Higgs [1, 2]. The ATLAS and CMS experiments are beginning to explore in detail the properties of the Higgs, including the various couplings to SM particles. Since invisible decays reduce the branching fraction to the (visible) SM final states, it is to be expected that  $\mathcal{B}(H \rightarrow \text{invisible})$  is strongly constrained. Indeed

<sup>4</sup> For a related isospin violating dark matter model see [98].

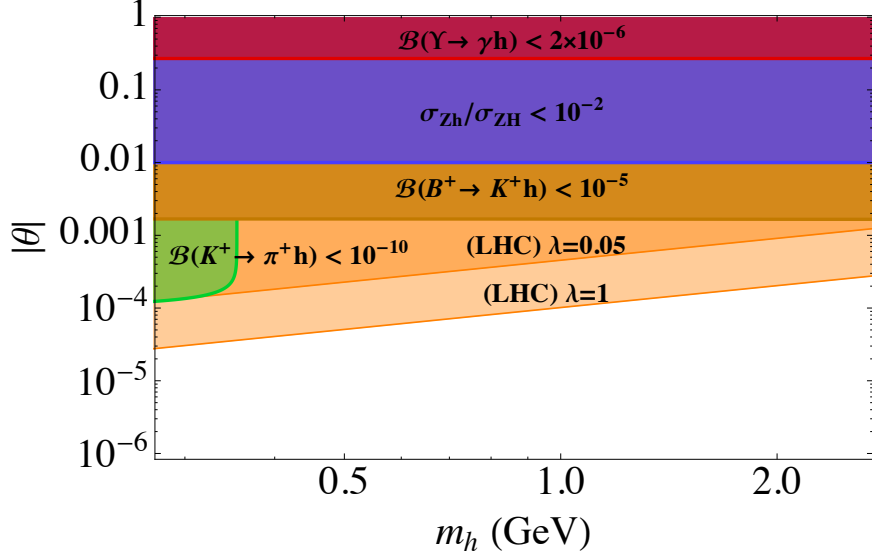


FIG. 6: Bounds on the  $(\theta, m_h)$  including invisible Higgs decays for different assumptions about the value of the quartic coupling  $\lambda$ .

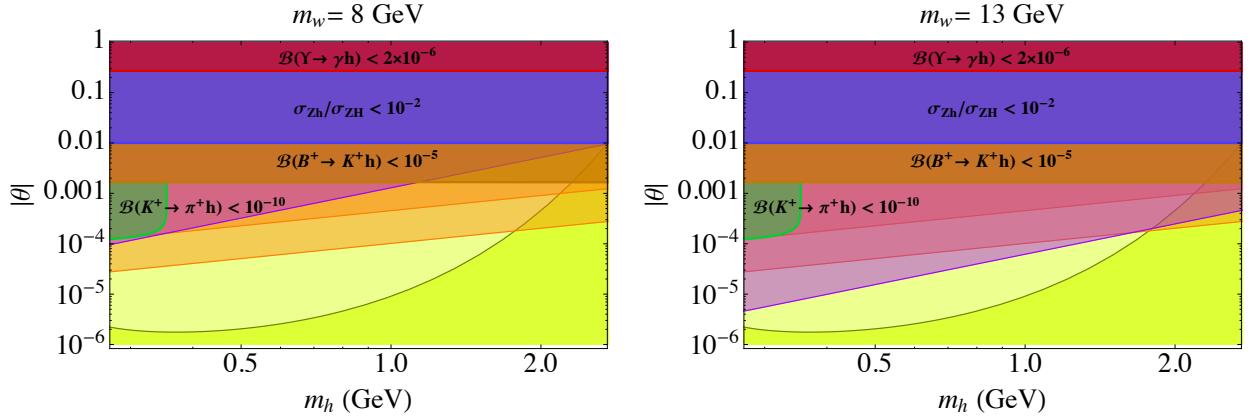


FIG. 7: Bounds on the  $(\theta, m_h)$  including limits on both invisible Higgs decays and direct dark matter detection for  $m_w = 8$  GeV and  $m_w = 13$  GeV.

$\mathcal{B}(H \rightarrow \text{invisible})$  is known to be less than about 19% at 95%CL [99–102]. For a Higgs width of about 4 MeV, the partial width for decay into unobserved particles is found to be

$$\Gamma_{H \rightarrow \text{invisible}} < 0.8 \text{ MeV}. \quad (43)$$

Four new processes contribute to the invisible decay of the Higgs boson. The new decay

modes and the corresponding decay rates are [60]

$$\begin{aligned}
\Gamma_{H \rightarrow \alpha\alpha} &= \frac{1}{32\pi} \left( \frac{g_\theta \langle \phi \rangle}{m_H^2 - m_h^2} \right)^2 m_H^3, \\
\Gamma_{H \rightarrow hh} &= \frac{1}{32\pi} \left( \frac{g_\theta \langle \phi \rangle}{m_H^2 - m_h^2} \right)^2 m_H^3, \\
\Gamma_{H \rightarrow \psi_\pm \psi_\pm} &= \frac{1}{16\pi} \left( \frac{f g_\theta \langle r \rangle \langle \phi \rangle}{m_H^2 - m_h^2} \right)^2 \sqrt{m_H^2 - 4m_\pm^2}.
\end{aligned} \tag{44}$$

The decay width of the Higgs into the hidden sector is then given by

$$\Gamma_{H \rightarrow \text{hidden}} = \frac{1}{16\pi} \left( \frac{g_\theta \langle \phi \rangle}{m_H^2 - m_h^2} \right)^2 m_H^3 + \frac{1}{8\pi} \left( \frac{f g_\theta \langle r \rangle \langle \phi \rangle}{m_H^2 - m_h^2} \right)^2 \sqrt{m_H^2 - 4m_w^2}. \tag{45}$$

Assuming  $m_H \gg m_h$ , this decay width is

$$\Gamma_{H \rightarrow \text{hidden}} = \frac{g_\theta^2 \langle \phi \rangle^2}{16\pi m_H} + \frac{g_\theta^2 \Delta m^2 \langle \phi \rangle^2}{32\pi m_H^3}. \tag{46}$$

Equation (46) can be written in terms of the mixing angle  $|\theta|$  and the quartic coupling of the hidden scalar  $\lambda$ ,

$$\Gamma_{H \rightarrow \text{hidden}} = \frac{\theta^2 m_H}{8\pi} \left[ \lambda \frac{m_H^2}{m_h^2} + f^2 \sqrt{1 - \frac{4m_w^2}{m_H^2}} \right]. \tag{47}$$

Equating (43) and (47) we obtain 90% C.L. exclusion contours in the  $(|\theta|, m_h)$  plane as a function of the free parameter  $\lambda$ ,

$$|\theta(\lambda)| < 1.27 \times 10^{-2} \left[ \lambda \frac{m_H^2}{m_h^2} + f^2 \sqrt{1 - \frac{4m_w^2}{m_H^2}} \right]^{-1/2}. \tag{48}$$

For the region of the parameter space of interest, the second term in (48) is negligible. In Fig. 6 we show the exclusion contours for the  $\lambda = 1$  and  $\lambda = 0.05$ . For smaller values of  $\lambda$ , bounds in the  $(|\theta|, m_h)$  plane are dominated by  $B$ -meson decays. Figure 7 displays the situation including bounds from direct detection experiments for two values of  $m_w$ . One sees that for  $m_w \gtrsim 13$  GeV the limit from LUX dominates the disallowed region.

## VII. CONCLUSIONS

In this article, we have examined Weinberg's Higgs portal model in light of a variety of experimental results. In the context of this model, we began by considering the excess of relativistic degrees of freedom,  $\Delta N_{\text{eff}}$ , induced by the weakly interacting Goldstone bosons,  $\alpha'$ , which decouple from SM particles in the late early universe. For masses of the hidden scalar in the range  $0.2 \text{ GeV} \lesssim m_h \lesssim 4 \text{ GeV}$ , the interaction rate of Goldstone bosons is dominated by resonant annihilation into fermion-antifermion pairs. In a recent calculation [61] this thermal annihilation rate was derived using Maxwell-Boltzmann statistics. We have verified

with a full expansion of the Bose-Einstein distribution that the leading term provides the results of [61], as well as negligible higher order terms. The decoupling temperature,  $T_{\alpha'}^{\text{dec}}$ , determines features of the contours in  $(|\theta|, m_h)$  parameter space, where  $\theta$  is the mixing angle in the Higgs sector. Following [59] we take as fiducial the contour for  $T_{\alpha'}^{\text{dec}} = m_\mu$  corresponding to  $N_{\text{eff}} = 3.39$ , which is a compromise between the number of effective neutrino species emerging from multi-parameter fits to Planck data in which the value  $h$  is, in one case, allowed to float in the fit, and in the second case is frozen to the value determined by the Hubble Space Telescope. This contour divides the parameter space into a lower region consistent with SM physics at the  $1\sigma$  level and an upper region requiring new physics at sub-fermi distance.

We then proceed to constrain the new physics regime using data from a variety of sources. First, we use data from BaBar [63–65], CLEO [66], BELLE [67], E787 [68], and E949 [69–71] on decays of heavy mesons with missing energy. Using results from searches for  $B^+ \rightarrow K^+ + \cancel{E}_T$  we derived an upper limit on the mixing angle that improves by one order of magnitude the latest bound derived in [82] from LEP limits on the production of invisibly-decaying Higgs bosons [78–81]. For  $m_h \lesssim 355$  MeV, measurements of  $K^+ \rightarrow \pi^+ + \cancel{E}_T$  further improve the upper limit on  $|\theta|$  by up to two orders of magnitude. The bounds resulting from our analysis rule out a significant part of the parameter space favored by CoGeNT [33–35] and CDMS II [36]. They are complementary (and comparable) to: (i) recent results from the ATLAS Collaboration [103] yielding bounds on a Higgs portal model in which the only interaction with the fermionic dark matter is through the SM Higgs [104–106]; (ii) bounds established from searches for  $B$  meson decay into charged leptons which have been used to constrain light scalar couplings in other Higgs portal models [107].

Next, we considered the implication of measurements from DM direct detection experiments. We extended the analysis developed in [60] to incorporate new results from CDM-Slite [40] and LUX [40]. We found exclusion regions on the  $(|\theta|, m_h)$  plane which are in agreement with those recently reported in [61]. We have shown that for light WIMPs,  $m_w \lesssim 9$  GeV, bounds from meson decay are more restrictive than limits from DM direct detection experiments. This is an interesting region to scrutinize, as signals have been reported both before [33–36] and after [108] the LUX bounds were published [40]. On the other hand, LUX measurements exclude heavy WIMPs,  $m_w \gtrsim 100$  GeV. For  $9$  GeV  $\lesssim m_w \lesssim 10$  GeV, the best limits come from CDM-Slite, while in the intermediate regions from  $10$  GeV  $\lesssim m_w \lesssim 55$  GeV and  $70$  GeV  $\lesssim m_w \lesssim 100$  GeV, LUX provides the best bounds. (In the region from about 55 GeV to 70 GeV the present analysis is not valid due to the presence of the Higgs resonance).

Finally, we considered constraints from LHC searches for invisible Higgs decays [99–102] for different assumptions about the Higgs quartic coupling,  $\lambda$ . These measurements further constrain the parameter space for  $m_w \lesssim 13$  GeV if the  $\lambda \gtrsim 0.05$ .

In summary, we have compressed the allowed parameter space for Weinberg’s Higgs portal model using a variety of complementary methods. Future measurements will deeply probe this model. Measurements by ATLAS and CMS with LHC running at 14 TeV center-of-mass energy will measure the Higgs couplings, and in conjunction with measurements from LHCb and NA62 [109], will provide a window to the low mass WIMP. Direct detection experiments like LUX and XENON1T [110] will either detect or constrain WIMPs with masses in the 10’s of GeV.



## Note Added

Shortly after this paper was written the SuperCDMS Collaboration presented new bounds on the low mass WIMP spin-independent interaction cross section [111]. These bounds, when translated into excluding regions of  $(\theta, m_h)$  plane, provide the most restrictive limits on the mixing angle for  $8 \text{ GeV} \lesssim m_w \lesssim 9 \text{ GeV}$ .

## Acknowledgments

This work was supported in part by the US NSF grants: CAREER PHY1053663 (LAA), PHY-0757959 (HG), PHY-1205854 (TCP), US DoE grant DE-FG05-85ER40226 (TJW), NASA NNX13AH52G (LAA, TCP), UWM RGI (BJV), and UWM Physics 2014 Summer Research Award (LHMdaS).

## Appendix A

Consider the annihilation process  $\alpha(k) \alpha(k') \rightarrow \bar{f}(p) f(p')$  in the center-of-mass frame, with the initial 3-momentum of the  $\alpha$  particles given as  $\mathbf{k} = -\mathbf{k}'$ , respectively. The differential cross section is given by

$$d\sigma = \frac{1}{2} \frac{|\overline{\mathcal{M}}|^2}{2k2k'} \frac{d^3p}{(2\pi)^2 2E_p} \frac{d^3p'}{2E_{p'}} \delta^{(3)}(\mathbf{p} + \mathbf{p}') \delta(2k - E_p - E_{p'}) . \quad (49)$$

Use of the spatial delta function allows us to write this result as

$$\begin{aligned} d\sigma &= \frac{|\overline{\mathcal{M}}|^2}{8k^2} \frac{d^3p}{(2\pi)^2 4E_p^2} \frac{1}{2} \delta(k - E_p) \\ &= \frac{|\overline{\mathcal{M}}|^2}{8k^2} \frac{pdE_p d\Omega}{(2\pi)^2 4E_p} \frac{1}{2} \delta(E_p - k) . \end{aligned} \quad (50)$$

After performing the integration over  $E_p$  we arrive at

$$d\sigma = \frac{1}{2} \frac{|\overline{\mathcal{M}}|^2}{32\pi k^2} \frac{d\Omega}{4\pi} \frac{\sqrt{k^2 - m_f^2}}{k} . \quad (51)$$

In terms of the invariant Mandelstam variable,  $s = (k + k')^2 = 4k^2$ , we can write the differential cross section as

$$d\sigma = \frac{|\overline{\mathcal{M}}|^2}{16\pi} \frac{d\Omega}{4\pi} \frac{\sqrt{s - 4m_f^2}}{s^{3/2}} . \quad (52)$$

We now turn to evaluate the invariant scattering amplitude. The Lagrangian describing the interaction of the Goldstone bosons with SM fields contains the Yukawa terms [60]

$$\frac{m_f}{\langle\phi\rangle} H \bar{f} f \cos\theta - \frac{m_f}{\langle\phi\rangle} h \bar{f} f \sin\theta , \quad (53)$$

and the terms coupling the Goldstone bosons with Higgs doublet and the  $CP$ -even scalar

$$\frac{\sin\theta}{\langle r \rangle} H (\partial\alpha)^2 + \frac{\cos\theta}{\langle r \rangle} h (\partial\alpha)^2 . \quad (54)$$

From (53) and (54) we get the Feynman rules for: the  $(\alpha, \alpha, H)$  vertex,  $-i2 \sin \theta (k \cdot k') / \langle r \rangle$ ; the  $(\alpha, \alpha, h)$  vertex,  $-i2 \cos \theta (k \cdot k') / \langle r \rangle$ ; the  $(H, \bar{f}, f)$  vertex,  $i m_f \cos \theta / \langle \phi \rangle$ ; and the  $(h, \bar{f}, f)$  vertex,  $i m_f \sin \theta / \langle \phi \rangle$ . All in all, the  $s$ -channel invariant amplitude of the process mediated by  $H$  and  $h$  can be expressed as

$$\mathcal{M} = \frac{2 \sin \theta \cos \theta}{\langle r \rangle \langle \phi \rangle} (k \cdot k') \left( \frac{m_H^2 - m_h^2}{(s - m_H^2)(s - m_h^2)} \right) \bar{u}(p') v(p). \quad (55)$$

Hence, for  $\theta \ll 1$ , the spin summed-average square amplitude is found to be

$$|\overline{\mathcal{M}}|^2 = \frac{4 m_f^2 g_\theta^2}{(s - m_H^2)^2 (s - m_h^2)^2} (k \cdot k')^2 4(p \cdot p' - m_f^2), \quad (56)$$

or in terms of invariant variables

$$|\overline{\mathcal{M}}|^2 = \frac{2 m_f^2 g_\theta^2}{(s - m_H^2)^2 (s - m_h^2)^2} s^2 (s - 4m_f^2). \quad (57)$$

Substituting (57) into (52) we obtain

$$\sigma_{\alpha\alpha} = \frac{4}{32\pi} \frac{m_f^2 g_\theta^2}{(s - m_H^2)^2 (s - m_h^2)^2} s^2 \left( 1 - \frac{4m_f^2}{s} \right)^{3/2}. \quad (58)$$

For phenomenological purposes, the poles need to be softened to a Breit-Wigner form by obtaining and utilizing the correct total widths of the resonances; *e.g.*, for  $\sqrt{s} \sim m_h$ ,

$$\frac{i}{s - m_h^2} \rightarrow \frac{i}{s - m_h^2 + i m_h \Gamma_h}. \quad (59)$$

After this is done, the scattering cross section becomes

$$\sigma_{\alpha\alpha} = \frac{4}{32\pi} \frac{m_f^2 \theta^2}{\langle r \rangle^2 \langle \phi \rangle^2} \frac{(m_H^2 - m_h^2)^2 + m_h^2 \Gamma_h^2}{(s - m_H^2)^2 [(s - m_h^2)^2 + m_h^2 \Gamma_h^2]} s^2 \left( 1 - \frac{4m_f^2}{s} \right)^{3/2}. \quad (60)$$

For  $m_h^2 \Gamma_h^2 \ll (m_H^2 - m_h^2)^2$ , we can drop the  $\Gamma_h$  term in the numerator to obtain

$$\sigma_{\alpha\alpha} = \frac{4}{32\pi} \frac{m_f^2 g_\theta^2}{(s - m_H^2)^2 [(s - m_h^2)^2 + m_h^2 \Gamma_h^2]} s^2 \left( 1 - \frac{4m_f^2}{s} \right)^{3/2}. \quad (61)$$

We have found that for the considerations in the present work, the cross section can be safely approximated by the single pole of the Narrow-Width Approximation. Namely, for  $m_h \Gamma_h \rightarrow 0$ , (61) can be rewritten as

$$\sigma_{\alpha\alpha} \approx \frac{4}{32} \frac{m_f^2 g_\theta^2}{(s - m_H^2)^2} s^2 \left( 1 - \frac{4m_f^2}{s} \right)^{3/2} \frac{\delta(s - m_h^2)}{m_h \Gamma_h}, \quad (62)$$

where we have used the relation

$$\lim_{\epsilon \rightarrow 0} \frac{\epsilon}{x^2 + \epsilon^2} = \pi \delta(x). \quad (63)$$

We now proceed to calculate the thermal-angular averages,

$$\langle \sigma_{\alpha\alpha} v_M \rangle = \frac{1}{n_\alpha^2} \int \frac{d^3 p_1}{(2\pi)^3} \frac{d^3 p_2}{(2\pi)^3} \sigma_{\alpha\alpha} v_M(s) \frac{1}{e^{E_1/T} - 1} \frac{1}{e^{E_2/T} - 1}, \quad (64)$$

where  $v_M$  is the is the Möller velocity [112]. Substituting the expansion of the Bose distribution,

$$\frac{1}{e^{E/T} - 1} = e^{-E/T} \sum_{n=0}^{\infty} e^{-nE/T}, \quad (65)$$

into (64) we obtain [97]

$$\langle \sigma_{\alpha\alpha} v_M \rangle = \frac{T}{8\pi^4 n_\alpha^2(T)} \sum_{k,n=0}^{\infty} \frac{1}{4\sqrt{(k+1)(n+1)}} \int_0^\infty \sigma_{\alpha\alpha} s \sqrt{s} K_1 \left( \frac{\sqrt{(k+1)(n+1)}s}{T} \right) ds,$$

with

$$n_\alpha = \int_0^\infty \frac{d^3 p}{(2\pi)^3} \frac{1}{e^{p/T} - 1} = \frac{\zeta(3)}{\pi^2} T^3. \quad (66)$$

Using the narrow width approximation to the annihilation cross section we have

$$\begin{aligned} \langle \sigma_{\alpha\alpha} v_M \rangle &= \frac{4m_f^2 g_\theta^2}{32^2 \zeta^2(3) T^5 \Gamma_h} \sum_{n,k=0}^{\infty} \frac{1}{\sqrt{(k+1)(n+1)}} \frac{m_h^6}{(m_h^2 - m_H^2)^2} \left(1 - \frac{4m_f^2}{m_h^2}\right)^{3/2} \\ &\times K_1 \left( \frac{\sqrt{(k+1)(n+1)}m_h}{T} \right), \end{aligned} \quad (67)$$

which under the assumption that  $m_h \ll m_H$  results in

$$\begin{aligned} \langle \sigma_{\alpha\alpha} v_M \rangle &= \frac{g_\theta^2}{256} \frac{m_f^2 m_h^6}{\zeta^2(3) T^5 m_H^4 \Gamma_h} \left(1 - \frac{4m_f^2}{m_h^2}\right)^{3/2} \sum_{n,k=0}^{\infty} \frac{1}{\sqrt{(k+1)(n+1)}} \\ &\times K_1 \left( \frac{\sqrt{(k+1)(n+1)}m_h}{T} \right). \end{aligned} \quad (68)$$

If we retain only the first term in the series we recover the result obtained in [61] using Maxwell-Boltzmann statistics,

$$\langle \sigma_{\alpha\alpha} v_M \rangle \approx \frac{g_\theta^2}{256} \frac{m_f^2 m_h^6}{\zeta^2(3) T^5 m_H^4 \Gamma_h} \left(1 - \frac{4m_f^2}{m_h^2}\right)^{3/2} K_1(m_h/T). \quad (69)$$

To check the accuracy of retaining only the first term of the series, we perform a numerical integration, which is shown in Fig. 8. The summation converges within the first  $N = 10$  terms of the series. For  $T \lesssim m_h$ , we find agreement at better than the 7% level between the 2<sup>nd</sup> Bessel function of the second kind and the double series,

$$\sum_{n,k=0}^{\infty} \frac{1}{\sqrt{(k+1)(n+1)}} K_1 \left( \frac{\sqrt{(k+1)(n+1)}m_h}{T} \right) \approx \zeta(3) K_2(m_h/T), \quad (70)$$

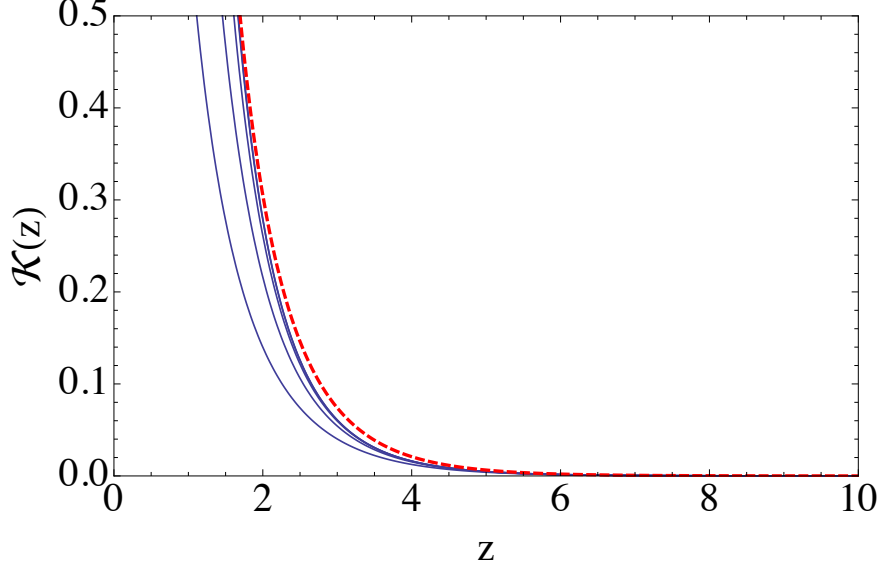


FIG. 8: The solid lines stand for  $\mathcal{K}(z) = \sum_{n,k=0}^N K_1(\sqrt{(k+1)(n+1)}z)/\sqrt{(k+1)(n+1)}$  as a function of  $z = m_h/T$ . From left to right  $N = 0, 1, 3, 10, 50$ . The sum quickly converges towards  $\zeta(3)K_2(z)$ , which is shown as a dashed curve.

as demonstrated in Fig. 8. This allows us to write an approximate expression for the double series and thus (68) becomes,

$$\langle \sigma_{\alpha\alpha} v_M \rangle \approx \frac{g_\theta^2}{256} \frac{m_f^2 m_h^6}{\zeta(3) T^5 m_H^4 \Gamma_h} \left( 1 - \frac{4m_f^2}{m_h^2} \right)^{3/2} K_2(m_h/T). \quad (71)$$

Multiplying (71) by the number density  $n_\alpha$  we obtain the interaction rate given in (19).

## Appendix B

For completeness, we briefly recall here the basics of the calculation of the  $w$  relic density [113]. The evolution of the number density  $n_w$  is governed by the Boltzmann transport equation

$$\dot{n}_w + 3Hn_w = -\langle \sigma_{ww} v_M \rangle (n_w^2 - n_{w_{\text{EQ}}}^2), \quad (72)$$

where  $x = m_w/T$ . In the non-relativistic limit, and in the Maxwell-Boltzmann approximation, the number density at thermal equilibrium is given by

$$n_{w_{\text{EQ}}} = g(x) \left( \frac{m_w^2}{2\pi} \right)^{3/2} x^{-3/2} e^{-x}. \quad (73)$$

We next introduce the yield variable  $Y \equiv n_w/s$ , where

$$s = g(x) \frac{2\pi^2}{45} m_w^3 x^{-3} \quad (74)$$

is the entropy density.<sup>5</sup> In particular,

$$Y_{\text{EQ}} \equiv \frac{n_{w\text{EQ}}}{s} = \frac{45}{\sqrt{32\pi^7}} x^{3/2} e^{-x}. \quad (75)$$

Using the conservation of entropy per comoving volume, it follows that

$$\dot{s} + 3Hs = 0, \quad (76)$$

or equivalently

$$\dot{x} = H(x)x, \quad (77)$$

where

$$H(x) = \sqrt{\frac{8\pi^3}{90}} \frac{1}{M_{\text{Pl}}} \sqrt{g(x)} m_w^2 x^{-2} = H(m_w) x^{-2}. \quad (78)$$

Equation (72) can now be expressed in terms of  $x$  and  $Y$  variables to obtain

$$\frac{dY}{dx} = -\frac{x \langle \sigma_{ww} v_M \rangle s}{H(m_w)} (Y^2 - Y_{\text{EQ}}^2), \quad (79)$$

where

$$\frac{x \langle \sigma_{ww} v_M \rangle s}{H(m_w)} = \sqrt{\frac{\pi}{45}} \sqrt{g(x)} m_w M_{\text{Pl}} \frac{\langle \sigma_{ww} v_M \rangle}{x^2}. \quad (80)$$

After reparametrizing the yield,  $Y = Y_{\text{EQ}} + \Delta$ , in (79) we obtain

$$\frac{dY_{\text{EQ}}}{dx} + \frac{d\Delta}{dx} = -\sqrt{\frac{\pi}{45}} \sqrt{g(x)} m_w M_{\text{Pl}} \frac{\langle \sigma_{ww} v_M \rangle}{x^2} \Delta (2Y_{\text{EQ}} + \Delta). \quad (81)$$

Near freeze out  $d\Delta/dx \approx 0$ , and so (81) simplifies to

$$\frac{1}{Y_{\text{EQ}}} \frac{dY_{\text{EQ}}}{dx} \approx -\sqrt{\frac{\pi}{45}} \sqrt{g(x_f)} m_w M_{\text{Pl}} \frac{\langle \sigma_{ww} v_M \rangle}{x_f^2} c(c+2) Y_{\text{EQ}}, \quad (82)$$

where we have taken  $\Delta(x_F) = cY_{\text{EQ}}(x_f)$  to define the freeze out time. Here,  $c$  is a constant of order one determined by matching the late-time and early-time solutions. Finally substitution of (75) into (82) leads to

$$e^{x_f} \approx c(c+2) \sqrt{\frac{45}{32\pi^6}} \sqrt{g(x_f)} m_w M_{\text{Pl}} \frac{\langle \sigma_{ww} v_M \rangle}{x_f^{1/2}}. \quad (83)$$

The freeze-out temperature  $x_f$  can be estimated through the iterative solution of (83), yielding

$$\begin{aligned} x_f &\approx \ln \left[ c(c+2) \sqrt{\frac{45}{32\pi^6}} \sqrt{g(x_f)} m_w M_{\text{Pl}} \langle \sigma_{ww} v_M \rangle \right] - \frac{1}{2} \ln x_f \\ &\approx \ln \left[ 0.1 \sqrt{g(x_f)} m_w M_{\text{Pl}} \langle \sigma_{ww} v_M \rangle \right] - \frac{1}{2} \ln \left( \ln \left[ 0.1 \sqrt{g(x_f)} m_w M_{\text{Pl}} \langle \sigma_{ww} v_M \rangle \right] \right). \end{aligned} \quad (84)$$

<sup>5</sup> If relativistic particles are present that have decoupled from the plasma, it is necessary to distinguish between two kinds of  $g$ :  $g_\rho$  which is associated with the total energy density, and  $g_s$  which is associated with the total entropy density. For our calculations we use  $g = g_\rho = g_s$ .

After freeze out the yield significantly departs from its equilibrium expression. Thus, to obtain the  $Y$  evolution for  $x \gg x_f$ , we can neglect the  $Y_{\text{EQ}}$  terms in (81) as the  $\Delta$  terms come to dominate,

$$\frac{d\Delta}{dx} = -\sqrt{\frac{\pi}{45}} \sqrt{g(x)} m_w M_{\text{Pl}} \frac{\langle \sigma_{ww} v_M \rangle}{x^2} \Delta^2 . \quad (85)$$

Upon solving for  $\Delta$  at today's value,  $x_0$ , we obtain

$$\frac{1}{Y(x_0)} = \frac{1}{\Delta(x_f)} + \sqrt{\frac{\pi}{45}} m_w M_{\text{Pl}} \int_{x_f}^{x_0} \sqrt{g(x)} \frac{\langle \sigma_{ww} v_M \rangle}{x^2} dx , \quad (86)$$

where we have taken  $\Delta(x_0) \approx Y(x_0)$ . Assuming that  $g(x)$  remains roughly constant over the integration range  $(x_f, x_0)$  and that  $\langle \sigma_{ww} v_M \rangle \propto x^{-n}$ , the first term in the right-hand-side of (86) becomes

$$\Delta^{-1}(x_f) = (c + 2) \sqrt{\frac{\pi}{45}} m_w M_{\text{Pl}} \sqrt{g(x_f)} \frac{\langle \sigma_{ww} v_M(x_f) \rangle}{x_f^2} , \quad (87)$$

whereas the second term is given by

$$\sqrt{\frac{\pi}{45}} m_w M_{\text{Pl}} \sqrt{g(x_f)} \int_{x_f}^{x_0} \frac{\langle \sigma_{ww} v_M \rangle}{x^2} dx \approx \sqrt{\frac{\pi}{45}} m_w M_{\text{Pl}} \sqrt{g(x_f)} \frac{\langle \sigma_{ww} v_M(x_f) \rangle}{(n + 1)x_f} . \quad (88)$$

Since the first term  $\propto \langle \sigma_{ww} v_M(x_f) \rangle / x_f^2$  and the second term  $\propto \langle \sigma_{ww} v_M(x_f) \rangle / x_f$ , for simplicity herein we neglect the  $\Delta^{-1}(x_f)$  contribution to (86). The present density of  $w$  is simply given by  $\rho_w = m_w n_w = m_w s_0 Y(x_0)$ , where  $s_0 = 2890.7(9) \text{ cm}^{-3} = 2.2211(4) \times 10^{-38} \text{ GeV}^3$  is the present entropy density (assuming three Dirac neutrino species) [27]. The relic density can finally be expressed in terms of the critical density

$$\Omega_{\text{DM}} h^2 = \frac{8\pi m_w s_0 Y(x_0)}{3M_{\text{Pl}}^2 (100 \text{ km/s/Mpc})^2} = 2.74 \times 10^8 \text{ GeV}^{-1} m_w Y(x_0) . \quad (89)$$

Substituting (86) into (89) we then have

$$\langle \sigma_{ww} v_M(x_f) \rangle = (n + 1) \frac{1.04 \times 10^9 \text{ GeV}^{-1} x_f}{\sqrt{g(x_f)} M_{\text{Pl}} \Omega_{\text{DM}} h^2} , \quad (90)$$

where we have taken  $T_0 = 2.7255 \text{ K}$  [27]. For  $\Delta m / m_w \rightarrow 0$ , we have  $n = 0$  leading to (40).

- 
- [1] G. Aad *et al.* [ATLAS Collaboration], Phys. Lett. B **716**, 1 (2012) [arXiv:1207.7214 [hep-ex]].
  - [2] S. Chatrchyan *et al.* [CMS Collaboration], Phys. Lett. B **716**, 30 (2012) [arXiv:1207.7235 [hep-ex]].
  - [3] G. Altarelli, arXiv:1308.0545 [hep-ph].
  - [4] S. Perlmutter *et al.* [Supernova Cosmology Project Collaboration], Astrophys. J. **517**, 565 (1999) [astro-ph/9812133].
  - [5] R. A. Knop *et al.* [Supernova Cosmology Project Collaboration], Astrophys. J. **598**, 102 (2003) [astro-ph/0309368].

- [6] M. Kowalski *et al.* [Supernova Cosmology Project Collaboration], *Astrophys. J.* **686**, 749 (2008) [arXiv:0804.4142 [astro-ph]].
- [7] A. G. Riess *et al.* [Supernova Search Team Collaboration], *Astron. J.* **116**, 1009 (1998) [astro-ph/9805201].
- [8] A. G. Riess *et al.* [Supernova Search Team Collaboration], *Astrophys. J.* **560**, 49 (2001) [astro-ph/0104455].
- [9] J. L. Tonry *et al.* [Supernova Search Team Collaboration], *Astrophys. J.* **594**, 1 (2003) [astro-ph/0305008].
- [10] D. N. Spergel *et al.* [WMAP Collaboration], *Astrophys. J. Suppl.* **148**, 175 (2003) [astro-ph/0302209].
- [11] E. Komatsu *et al.* [WMAP Collaboration], *Astrophys. J. Suppl.* **192**, 18 (2011) [arXiv:1001.4538 [astro-ph.CO]].
- [12] G. Hinshaw *et al.* [WMAP Collaboration], arXiv:1212.5226 [astro-ph.CO].
- [13] A. G. Riess *et al.*, *Astrophys. J.* **699**, 539 (2009) [arXiv:0905.0695 [astro-ph.CO]].
- [14] A. G. Riess *et al.*, *Astrophys. J.* **730**, 119 (2011) [Erratum *ibid.* **732**, 129 (2011)] [arXiv:1103.2976 [astro-ph.CO]].
- [15] K. Abazajian *et al.* [SDSS Collaboration], *Astron. J.* **126**, 2081 (2003) [astro-ph/0305492].
- [16] M. Tegmark *et al.* [SDSS Collaboration], *Phys. Rev. D* **69**, 103501 (2004) [astro-ph/0310723].
- [17] K. N. Abazajian *et al.* [SDSS Collaboration], *Astrophys. J. Suppl.* **182**, 543 (2009) [arXiv:0812.0649 [astro-ph]].
- [18] W. J. Percival *et al.* [SDSS Collaboration], *Mon. Not. Roy. Astron. Soc.* **401**, 2148 (2010) [arXiv:0907.1660 [astro-ph.CO]].
- [19] P. A. R. Ade *et al.* [Planck Collaboration], arXiv:1303.5076 [astro-ph.CO].
- [20] J. L. Feng, *Ann. Rev. Astron. Astrophys.* **48**, 495 (2010) [arXiv:1003.0904 [astro-ph.CO]].
- [21] G. Steigman and M. S. Turner, *Nucl. Phys. B* **253**, 375 (1985).
- [22] B. W. Lee and S. Weinberg, *Phys. Rev. Lett.* **39**, 165 (1977).
- [23] D. A. Dicus, E. W. Kolb and V. L. Teplitz, *Phys. Rev. Lett.* **39**, 168 (1977) [Erratum-*ibid.* **39**, 973 (1977)].
- [24] E. W. Kolb and K. A. Olive, *Phys. Rev. D* **33**, 1202 (1986) [Erratum-*ibid.* **D 34**, 2531 (1986)].
- [25] R. J. Scherrer and M. S. Turner, *Phys. Rev. D* **33**, 1585 (1986) [Erratum-*ibid.* **D 34**, 3263 (1986)].
- [26] G. Steigman, B. Dasgupta and J. F. Beacom, *Phys. Rev. D* **86**, 023506 (2012) [arXiv:1204.3622 [hep-ph]].
- [27] J. Beringer *et al.* [Particle Data Group Collaboration], *Phys. Rev. D* **86**, 010001 (2012).
- [28] R. Bernabei *et al.*, *Phys. Lett. B* **424** 195 (1998).
- [29] R. Bernabei *et al.*, *Eur. Phys. J. C* **67** 39 (2010) [arXiv:1002.1028 [astro-ph.GA]].
- [30] A. K. Drukier, K. Freese and D. N. Spergel, *Phys. Rev. D* **33** 3495 (1986).
- [31] K. Freese, J. A. Frieman and A. Gould, *Phys. Rev. D* **37** 3388 (1988).
- [32] G. Angloher *et al.*, *Eur. Phys. J. C* **72**, 1971 (2012) [arXiv:1109.0702 [astro-ph.CO]].
- [33] C. E. Aalseth *et al.* [CoGeNT Collaboration], *Phys. Rev. Lett.* **106**, 131301 (2011) [arXiv:1002.4703 [astro-ph.CO]].
- [34] C. E. Aalseth *et al.* [CoGeNT Collaboration], *Phys. Rev. Lett.* **107** 141301 (2011) [arXiv:1106.0650 [astro-ph.CO]].
- [35] C. E. Aalseth *et al.* [CoGeNT Collaboration], *Phys. Rev. D* **88**, 012002 (2013) [arXiv:1208.5737 [astro-ph.CO]].
- [36] R. Agnese *et al.* [CDMS Collaboration], *Phys. Rev. Lett.* **111**, 251301 (2013) [arXiv:1304.4279]

- [hep-ex]].
- [37] J. Angle *et al.* [XENON10 Collaboration], Phys. Rev. Lett. **107**, 051301 (2011) [arXiv:1104.3088 [astro-ph.CO]].
  - [38] E. Aprile *et al.* [XENON100 Collaboration], Phys. Rev. Lett. **107**, 131302 (2011) [arXiv:1104.2549 [astro-ph.CO]].
  - [39] R. Agnese *et al.*, arXiv:1309.3259 [physics.ins-det].
  - [40] D. S. Akerib *et al.* [LUX Collaboration], arXiv:1310.8214 [astro-ph.CO].
  - [41] A. Kurylov and M. Kamionkowski, Phys. Rev. D **69**, 063503 (2004) [hep-ph/0307185].
  - [42] F. Giuliani, Phys. Rev. Lett. **95**, 101301 (2005) [hep-ph/0504157].
  - [43] J. L. Feng, J. Kumar, D. Marfatia and D. Sanford, Phys. Lett. B **703**, 124 (2011) [arXiv:1102.4331 [hep-ph]].
  - [44] M. T. Frandsen, F. Kahlhoefer, C. McCabe, S. Sarkar and K. Schmidt-Hoberg, JCAP **1307**, 023 (2013) [arXiv:1304.6066 [hep-ph]].
  - [45] J. L. Feng, J. Kumar and D. Sanford, Phys. Rev. D **88**, 015021 (2013) [arXiv:1306.2315 [hep-ph]].
  - [46] M. I. Gresham and K. M. Zurek, arXiv:1311.2082 [hep-ph].
  - [47] E. Del Nobile, G. B. Gelmini, P. Gondolo and J. -H. Huh, arXiv:1311.4247 [hep-ph].
  - [48] V. Cirigliano, M. L. Graesser, G. Ovanessian and I. M. Shoemaker, arXiv:1311.5886 [hep-ph].
  - [49] J. Dunkley *et al.*, Astrophys. J. **739**, 52 (2011) [arXiv:1009.0866 [astro-ph.CO]].
  - [50] R. Keisler *et al.*, Astrophys. J. **743**, 28 (2011) [arXiv:1105.3182 [astro-ph.CO]].
  - [51] J. Hamann, JCAP **1203**, 021 (2012) [arXiv:1110.4271 [astro-ph.CO]].
  - [52] M. Benetti, M. Gerbino, W. H. Kinney, E. W. Kolb, M. Lattanzi, A. Melchiorri, L. Pagano and A. Riotto, arXiv:1303.4317 [astro-ph.CO].
  - [53] G. Steigman, Adv. High Energy Phys. **2012**, 268321 (2012) [arXiv:1208.0032 [hep-ph]].
  - [54] G. Steigman, D.N. Schramm and J.E. Gunn, Phys. Lett. B **66**, 202 (1977).
  - [55] R. Schabinger and J. D. Wells, Phys. Rev. D **72**, 093007 (2005) [hep-ph/0509209].
  - [56] B. Patt and F. Wilczek, hep-ph/0605188.
  - [57] V. Barger, P. Langacker, M. McCaskey, M. J. Ramsey-Musolf and G. Shaughnessy, Phys. Rev. D **77**, 035005 (2008) [arXiv:0706.4311 [hep-ph]].
  - [58] V. Barger, P. Langacker, M. McCaskey, M. Ramsey-Musolf and G. Shaughnessy, Phys. Rev. D **79**, 015018 (2009) [arXiv:0811.0393 [hep-ph]].
  - [59] S. Weinberg, Phys. Rev. Lett. **110**, **241301** (2013) [arXiv:1305.1971 [astro-ph.CO]].
  - [60] L. A. Anchordoqui and B. J. Vlcek, Phys. Rev. D **88**, 043513 (2013) [arXiv:1305.4625 [hep-ph]].
  - [61] C. Garcia-Cely, A. Ibarra and E. Molinaro, arXiv:1310.6256 [hep-ph].
  - [62] C. Bird, P. Jackson, R. V. Kowalewski and M. Pospelov, Phys. Rev. Lett. **93**, 201803 (2004) [hep-ph/0401195].
  - [63] B. Aubert *et al.* [BaBar Collaboration], Phys. Rev. Lett. **94**, 101801 (2005) [hep-ex/0411061].
  - [64] P. del Amo Sanchez *et al.* [BaBar Collaboration], Phys. Rev. D **82**, 112002 (2010) [arXiv:1009.1529 [hep-ex]].
  - [65] J. P. Lees *et al.* [BaBar Collaboration], Phys. Rev. D **87**, 112005 (2013) [arXiv:1303.7465 [hep-ex]].
  - [66] T. E. Browder *et al.* [CLEO Collaboration], Phys. Rev. Lett. **86**, 2950 (2001) [hep-ex/0007057].
  - [67] O. Lutz *et al.* [Belle Collaboration], Phys. Rev. D **87**, 111103 (2013) [arXiv:1303.3719 [hep-ex]].



- [68] S. Adler *et al.* [E787 Collaboration], Phys. Rev. Lett. **88**, 041803 (2002) [hep-ex/0111091].
- [69] V. V. Anisimovsky *et al.* [E949 Collaboration], Phys. Rev. Lett. **93**, 031801 (2004) [hep-ex/0403036].
- [70] S. Adler *et al.* [E949 and E787 Collaborations], Phys. Rev. D **77**, 052003 (2008) [arXiv:0709.1000 [hep-ex]].
- [71] A. V. Artamonov *et al.* [BNL-E949 Collaboration], Phys. Rev. D **79**, 092004 (2009) [arXiv:0903.0030 [hep-ex]].
- [72] P. del Amo Sanchez *et al.* [BaBar Collaboration], Phys. Rev. Lett. **107**, 021804 (2011) [arXiv:1007.4646 [hep-ex]].
- [73] F. Wilczek, Phys. Rev. Lett. **39**, 1304 (1977).
- [74] M. I. Vysotsky, Phys. Lett. B **97**, 159 (1980).
- [75] P. Nason, Phys. Lett. B **175**, 223 (1986).
- [76] H. Goldberg and Z. Ryzak, Phys. Lett. B **218**, 348 (1989).
- [77] F. P. Huang, C. S. Li, D. Y. Shao and J. Wang, arXiv:1307.7458 [hep-ph].
- [78] R. Barate *et al.* [ALEPH Collaboration], Phys. Lett. B **466**, 50 (1999).
- [79] J. Abdallah *et al.* [DELPHI Collaboration], Eur. Phys. J. C **32**, 475 (2004) [hep-ex/0401022].
- [80] P. Achard *et al.* [L3 Collaboration], Phys. Lett. B **609**, 35 (2005) [hep-ex/0501033].
- [81] G. Abbiendi *et al.* [OPAL Collaboration], Phys. Lett. B **682**, 381 (2010) [arXiv:0707.0373 [hep-ex]].
- [82] K. Cheung, W. -Y. Keung and T. -C. Yuan, arXiv:1308.4235 [hep-ph].
- [83] G. Buchalla, G. Hiller and G. Isidori, Phys. Rev. D **63**, 014015 (2000) [hep-ph/0006136].
- [84] M. Bartsch, M. Beylich, G. Buchalla and D. -N. Gao, JHEP **0911**, 011 (2009) [arXiv:0909.1512 [hep-ph]].
- [85] A. Abada and S. Nasri, Phys. Rev. D **85**, 075009 (2012) [arXiv:1201.1413 [hep-ph]].
- [86] M. Bargiotti *et al.*, Riv. Nuovo Cim. **23N3**, 1 (2000) [hep-ph/0001293].
- [87] G. Buchalla and A. J. Buras, Nucl. Phys. B **548**, 309 (1999) [hep-ph/9901288].
- [88] J. Brod and M. Gorbahn, Phys. Rev. D **78**, 034006 (2008) [arXiv:0805.4119 [hep-ph]].
- [89] J. Brod, M. Gorbahn and E. Stamou, Phys. Rev. D **83**, 034030 (2011) [arXiv:1009.0947 [hep-ph]].
- [90] K. Ghorbani and H. Ghorbani, arXiv:1301.0919 [hep-ph].
- [91] M. Beltran, D. Hooper, E. W. Kolb and Z. C. Krusberg, Phys. Rev. D **80**, 043509 (2009) [arXiv:0808.3384 [hep-ph]].
- [92] S. Baek and H. Okada, arXiv:1311.2380 [hep-ph].
- [93] D. Hooper and T. R. Slatyer, arXiv:1302.6589 [astro-ph.HE].
- [94] W. -C. Huang, A. Urbano and W. Xue, arXiv:1307.6862 [hep-ph].
- [95] N. Okada and O. Seto, arXiv:1310.5991 [hep-ph].
- [96] W. -C. Huang, A. Urbano and W. Xue, arXiv:1310.7609 [hep-ph].
- [97] P. Gondolo and G. Gelmini, Nucl. Phys. B **360**, 145 (1991).
- [98] N. Okada and O. Seto, Phys. Rev. D **88**, 063506 (2013) [arXiv:1304.6791 [hep-ph]].
- [99] J. R. Espinosa, M. Muhlleitner, C. Grojean and M. Trott, JHEP **1209**, 126 (2012) [arXiv:1205.6790 [hep-ph]].
- [100] K. Cheung, J. S. Lee and P. -Y. Tseng, JHEP **1305**, 134 (2013) [arXiv:1302.3794 [hep-ph]].
- [101] P. P. Giardino, K. Kannike, I. Masina, M. Raidal and A. Strumia, arXiv:1303.3570 [hep-ph].
- [102] J. Ellis and T. You, arXiv:1303.3879 [hep-ph].
- [103] G. Aad *et al.* [ATLAS Collaboration], arXiv:1402.3244 [hep-ex].
- [104] S. Kanemura, S. Matsumoto, T. Nabeshima and N. Okada, Phys. Rev. D **82**, 055026 (2010)

- [arXiv:1005.5651 [hep-ph]].
- [105] P. J. Fox, R. Harnik, J. Kopp and Y. Tsai, *Phys. Rev. D* **85**, 056011 (2012) [arXiv:1109.4398 [hep-ph]].
- [106] A. Djouadi, O. Lebedev, Y. Mambrini and J. Quevillon, *Phys. Lett. B* **709**, 65 (2012) [arXiv:1112.3299 [hep-ph]].
- [107] K. Schmidt-Hoberg, F. Staub and M. W. Winkler, *Phys. Lett. B* **727** (2013) 506-510 [arXiv:1310.6752 [hep-ph]].
- [108] C. E. Aalseth *et al.* [CoGeNT Collaboration], arXiv:1401.3295 [astro-ph.CO].
- [109] M. Moulson [for the NA62 Collaboration], *PoS KAON* **13**, 013 (2013) [arXiv:1306.3361 [hep-ex]].
- [110] E. Aprile [XENON1T Collaboration], arXiv:1206.6288 [astro-ph.IM].
- [111] R. Agnese *et al.* [SuperCDMS Collaboration], arXiv:1402.7137 [hep-ex].
- [112] T. J. Weiler, *AIP Conf. Proc.* **1534**, 165 (2012) [arXiv:1301.0021 [hep-ph]].
- [113] E. W. Kolb and M. S. Turner, *The Early Universe*, *Front. Phys.* **69**, 1 (1990).